ISSN 2616-5767 Vol.9, Issue 1: 24-32, DOI: 10.25236/AJETS.2026.090103

Research on the Influence of Delay Time between Layered Blasting Holes on Blasting Effect

Gui Wei[1,a], Zong Qi[1,b,*]

[1]School of Civil Engineering and Architecture, Anhui University of Science and Technology, Huainan, China
[a]3290864685@qq.com, [b]qzong@aust.edu.cn
[*]Corresponding author

Abstract: *In the process of tunnel blasting and tunneling construction, the blasting effect is often poor due to the bedding and weak surfaces of the surrounding rock. The results show that the blasting effect of the computational model with a delay of 4 ms between the two holes is the best under the action of stress waves, and the peak attenuation of stress on both sides of the bedding surface closest to the post-blasting hole is the smallest, only 48%, and the design requirements of the delayed detonation time between the pores of the bedding rock mass are consistent with that of the complete rock mass. That is, when the first burst stress wave completes the expansion stage of rock fractures, the blasting effect will be better when the burst hole is detonated again.*

Keywords: *Tunnel blasting; bedding; delay time; blasting effect*

1. Introduction

With the continuous progress of science and technology, construction equipment is also constantly updated and iterated, and tunnel boring construction is more inclined to use mechanical rock breaking, but in the construction of surrounding rock under complex conditions such as bedding and weak surfaces, drilling and blasting method is still a more efficient and economical method. In engineering practice, the blasting effect is subject to factors such as bedding, cracks, and blasting parameters, which often leads to high bulk rate, serious over-under-excavation, and low blast hole utilization, which reduces the construction quality and efficiency[1].

In the construction of tunnel blasting, multi-section blast holes are usually used and different delay times are set to reduce the sandwiching effect of rock and improve the efficiency of blasting rock breaking, but when the surrounding rock blasting with bedding is blasted, the blasting stress wave will be reflected and transmitted in the bedding plane, and at the same time, the bedding surface will be crushed, slip and other phenomena, and the blasting mechanism is very different from the blasting of the complete rock mass, so many scholars have carried out relevant research on the blasting of layered rock mass. Agrawal Anurag et al.[2] proposed a blasting technique based on delay mode and table orientation to reduce the blasting vibration in coalfields with layered surfaces. YANG Guoliang et al.[3] conducted blasting tests on shale cube specimens at four different slit angles using a slit packet to explore the blasting fracture mechanism of bedding shale under directional fracture control blasting. Chen Yekai et al.[4] optimized the blasting design by accurately simulating the damage area caused by blasting excavation of the bedding slope to ensure the stability of the slope under blasting load. WANG Haiyang et al.[5] studied the influence of the position of the bedding surface and its medium properties on the propagation of hydraulic blasting stress waves, and found that the smaller the distance between the bedding surface and the blast source, the more obvious the inhibition effect on the propagation of blasting stress waves and crack propagation, the greater the difference in the performance between the bedding surface medium and the rock mass, and the more serious the attenuation of stress waves on the bedding surface. YANG Renshu et al.[6] studied the dynamic mechanical behavior of crack cracking and propagation through bedding blasting through the blast hole under high stress through model experiments, and found that with the increase of the angle between the bedding direction and the static stress direction, the propagation time of the main crack burst decreased, the maximum deflection angle increased, and the propagation path became more tortuous.

The above research focuses on the influence of bedding on the blasting mechanism in order to pursue efficient blasting construction. Based on this, according to the numerical simulation method, the blasting

ISSN 2616-5767 Vol.9, Issue 1: 24-32, DOI: 10.25236/AJETS.2026.090103

effects of layered rock mass and complete rock mass with different delay times are calculated and compared according to the time required for stress waves to complete different stages, which can provide reference for similar projects.

2. Material model and parameter determination

2.1 Explosives and air parameters

Using the No. 2 rock emulsification explosive, the high-energy explosive model *MAT_HIGH_EXPLOSIVE_BURN is adopted in LS-DYNA, and the detonation pressure P is defined as a function of the relative volume V and the internal energy parameter E0 using the JWL equation of state:

$$P = \left(1 - \frac{\omega}{R_1 V}\right) e^{R_1 V} + B\left(1 - \frac{\omega}{R_2 V}\right) e^{R_2 V} + \frac{\omega}{E_0 V} \tag{1}$$

Where, P is the detonation pressure; V is the relative volume, which defaults to 1; E_0 is the internal energy parameter; A, B, R_1 and R_2 are the material characteristic parameters. ω is the Greene-Eisen parameter. The parameters of the JWL equation of state for explosives are shown in Table 1.

The air material uses the *MAT_NULL model, and its equation of state is represented by the linear polynomial *EOS_LINER_POLYNOMIAL:

$$P = C_0 + C_1 V + C_2 V^2 + C_3 V^3 + (C_4 + C_5 V + C_6 V^2) E_0 \tag{2}$$

Where, C_0~C_6 is the air material parameter, C_4=C_5=0.4, and the other parameters from C_0 to C_6 are constants. E_0=0.25 MJ/m^3; V=1.0; The rest of the parameters are 0.

Table 1: Parameters of JWL equation of state for emulsified explosives

Parameters	ρ_0/ (g cm^{-3})	VOD/ (m·s^{-1})	P_{CJ}/ 10^2 GPa	E_0/ GPa	A/ GPa	B/ GPa	R_1	R_2	ω
Numerical value	1.1	4500	9.7	4.12	214	0.182	4.2	0.9	0.15

2.2 Rock and joint parameters

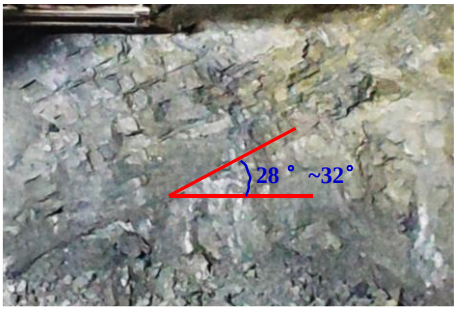

Figure 1: Tunnel section

Figure 1 shows the blasting construction section of a tunnel, and it can be found that the rock mass is distributed in layers with an inclination angle of about 30 °, and the basic physical and mechanical properties of the sandstone are sampled from the tunnel face and processed into standard specimens, and the basic physical and mechanical properties of sandstone are tested, and the basic physical and mechanical parameters of sandstone are obtained as shown in Table 2.

Table 2: Basic physical and mechanical parameters of sandstone

Parameters	ρ_0/ (g cm^{-3})	c_0/ (m·s^{-1})	f_c/ MPa	f_t/ MPa	E/ GPa	PR
Numerical value	2.73	4852	119.3	5.17	16.2	0.17

The rock adopts the RHT model, which creatively proposes an constitutive model of tensile compression damage, and describes the degree of rock damage by the damage parameter D($0<D<1$). When $D\geq0.8$, the rock is completely destroyed; when $D\leq D<0.8$ is 0.6, the rock loses its self-stabilization ability due to strong impact, resulting in macroscopic cracks. When $0.2\leq D<0.6$, the rock was only slightly damaged, and reticulated cracks appeared inside[7].

ISSN 2616-5767 Vol.9, Issue 1: 24-32, DOI: 10.25236/AJETS.2026.090103

The main parameters of the RHT model are divided into P-α equation of state-related parameters, strength-related parameters and damage parameters, and the P-α equation of state is

$$P = A_1\mu + A_2\mu_2 + A_3\mu_3 + (B_0+B_1\mu)\rho_0 e, \mu>0 \tag{3}$$

$$P = T_1\mu + T_2\mu^2 + B_0\rho_0 e, \mu<0 \tag{4}$$

Where, $\mu=P(\rho^*\alpha)/\rho_0-1$; ρ_0 is the initial density of the rock; ρ^* is the density of the rock when it is compressed; e is the initial internal energy of the rock; A_1, A_2 and A_3 are the Hugoniot polynomial coefficients; B_0, B_1, T_1 and T_2 are the parameters of the equation of state. $\mu>0$ causes the compressive volume of the rock to shrink, and vice versa, the tensile volume expands. $A_1=\rho_0 c_0^2$, $A_2=A_1(2s-1)$, $A_3=A_1(3s^2-4s+1)$, $B_0=B_1=\gamma_0=(2s-1)$, $T_1=A_1$, $T_2=0$, $s=0.9$[1]。

The corresponding porosity α of rocks can be expressed as:

$$\alpha = 1+(\alpha_0-1)\left[\frac{P_{\text{comp}}-P}{P_{\text{comp}}-P_{\text{el}}}\right]^n \tag{5}$$

Where, P_{el} is the pressure when the rock pores begin to be crushed; P_{comp} is the pressure when the rock pores are completely crushed, $P_{\text{el}}=f_c/3$; that is, the pressure when the rock is in a compact state; n is the compression exponent.

According to Li[8], the compressive strain index $\beta_c=4/(20+3f_c)$ and the tensile strain index $\beta_t=2/(20+f_c)$ can be obtained. The shear strength ratio is $f_s^*=f_s/f_c$, and the tensile compressive strength ratio is $f_t^*=f_t/f_c$; Parameters A and N are obtained according to the expression of the failure surface at $3P_0^*\geq F$, i.e., Eqa. (1); When the material is in quasi-static loading conditions, F_r takes 1, and Eqa. (6) is transformed into Eqa. (7).

$$\sigma f^*(P^*,F_r) = A(P^*-F_r/3+(A/F_r)^{-1/N})^N \tag{6}$$

$$\sigma f^* = A(P^*-1/3+A^{-1/N})^N \tag{7}$$

Where, P^* is the normalized pressure, $P^*=P/f_c$ (P^* dimensionless). Using the empirical formula and fitting analysis of Eqa. (7), it is obtained that A and N, Q_0 and B have little effect on rock stress-strain, and the relevant parameters of concrete are cited as tensile and compressive yield surface parameters g_t^* and g_c^*, and the residual stress strength parameters, exponents A_f and N_f[9].

The damage parameter D is defined as the cumulative of the plastic strain ε_p:

$$D = \sum \frac{d\varepsilon_p}{\varepsilon_p^f} \tag{8}$$

Where, ε_p^f is the plastic strain of the rock during failure and failure; εm p is the minimum failure effect variable; The damage parameters D_1 and D_2 can be taken from the initial values of 0.04 and 1.0; ε_0^t, ε_0^c, ε_t, ε_c are the values given in the original literature of the RHT model, and there is no need to change them.

Based on the above, the main parameters of the rock RHT model are shown in Table 3.

Table 3: Main parameters of sandstone RHT constitutive model [10]

f_c/ MPa	G/ GPa	ρ_0/ (g cm^{-3})	P_{el}/ MPa	α_0	β_c	β_t	B_0	B_1	A_1/ GPa	A_2/ GPa	A_3/ GPa
119.3	7.42	2.73	39.7	1.09	0.01	0.014	0.9	0.9	64.3	57.8	-5.9
T_1/ GPa	A_f	n	P_{comp}/ GPa	g^*_t	g^*_c	Q_0	ζ	N	f^*_t	f^*_s	A
64.3	1.6	3	0.6	0.7	0.57	0.68	0.5	0.61	0.043	0.53	3.05

The plastic behavior of isotropic hardening and follow-up hardening of bedding was described by *PLASTIC_KINEMATIC model[11], and the parameters are shown in Table 4.

Table 4: Physical parameters of the layer [5]

ρ/ (g cm^{-3})	E/ GPa	PR	E_{tan}/ GPa	σ_{Yield}/ MPa
2.1	15	0.34	1	19

ISSN 2616-5767 Vol.9, Issue 1: 24-32, DOI: 10.25236/AJETS.2026.090103

3. Design of delayed detonation calculation model

3.1 Delay time calculation

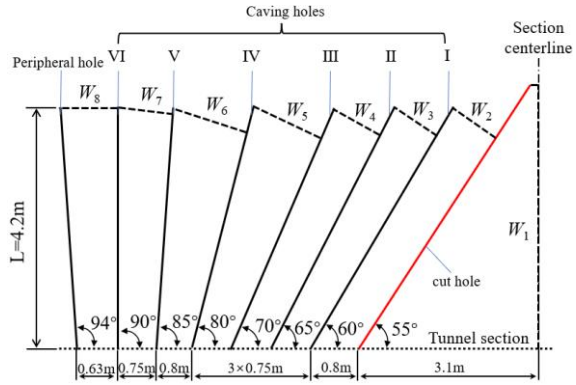

Figure 2: Layout of the blasting hole layout of the bedding tunnel

In tunnel blasting, for grooving holes and collapsed holes, it is usually necessary to set a certain delay time, and the inter-hole delay mechanism of the surrounding hole is different from the above-mentioned blast holes, which often requires the smallest or no delay between the peripheral holes, so that the cracks extend radially along the blast holes and improve the forming quality of the surrounding holes. As shown in Figure 2, the layout plan of the blast holes in the middle layered tunnel in Figure 1 (tunneling I.~VI. represents different sections of blast holes, and a certain delay time is set), and the delay time between different sections of the blast hole in the complete rock mass is calculated[12]

$$S_i = \frac{W_i}{C_P} + \frac{W_i}{V_c \cos\beta/2} + \frac{(0.5 \sim 0.8)W_i}{V_P} \tag{9}$$

Where, C_P is the longitudinal wave velocity of the rock; V_c is the average velocity of fracture propagation in rock, generally V_c=400~500 m/s; β is the angle of the blasting funnel cone, generally 70~120°; V_p is the average movement speed of rock blocks, V_p=5~10 m/s; W_i (i=1~8) represents the resistance lines of different sections of the blast holes, and the calculated value of the delay between different sections of the blast holes S_i (i=1~8) is calculated respectively, as shown in Table 4 (S_1 represents the delay of the detonator in the grooved hole, S_2 represents the delay of the detonator between the tunneling I and the grooved hole, and so on, calculated according to the compromise value of each parameter).

Table 5: Delay time between the minimum resistance line and different sections of the blast hole

Resistance line	W_1	W_2	W_3	W_4	W_5	W_6	W_7	W_8
Unit/ m	3.686	1.152	1.147	1.016	1.434	1.263	1.113	0.924
Delay time	S_1	S_2	S_3	S_4	S_5	S_6	S_7	S_8
Unit/ ms	0	86.1	85.1	84.7	86.1	85.5	85.0	84.8

It can be found that the results presented in Table 5 are mainly determined by the third item of Eqa. (9), which is also relatively easy to understand, and the process of blasting rock is mainly divided into two stages, namely, the dynamic action of explosive stress waves (initial stage) and the quasi-static action process of explosive gases (main stage)[13].

3.2 Design of calculation working conditions

In order to facilitate the research, only the first two terms in Eqa. (9) are considered, the value of the unified W_i is 1 m, and the value of the first term (the time of stress wave propagation to the free surface) is calculated to be about 0.2 ms, and the value range of the second term is about 2.44~4.8 ms. The value range of stress wave propagation and fracture expansion time is about 2.64~5.0 ms, so the delay between holes is 0 ms, 0.2 ms, 1 ms, 2 ms, 3 ms and 4 ms, respectively, and the overall calculation time is 5 ms. The distribution characteristics of the rock strata of the typical section of the tunnel are selected, specifically the spacing between the layers of the bedding surface is 20 cm, the bedding thickness is 0.25

ISSN 2616-5767 Vol.9, Issue 1: 24-32, DOI: 10.25236/AJETS.2026.090103

cm, and the bedding inclination angle is 30 °, and the numerical calculation model of the double hole is established as shown in Figure 3, and the displacement constraints are added above and below to simulate the plane strain problem, the 1# blast hole is close to the free surface, representing the first blast hole, and the 2# blast hole represents the post-blast hole, so as to simulate the effect of delayed detonation in the actual working condition, the diameter of the blast hole is 42 mm, the diameter of the coil is 32 mm, and the hole spacing is 1 m. The rocks are described using Lagrange grids, using Lagrange elements; The explosives and air are described by using Euler cells, and the rock and air are overlapped by the keyword *CONSTRAINED_LAGRANGE_IN_SOLID to achieve the effect of fluid-structure coupling.

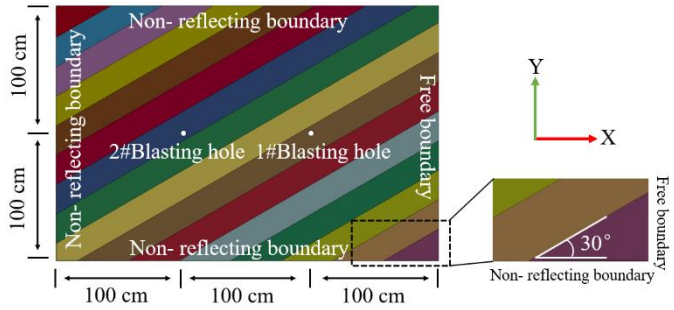

Figure 3: Numerical calculation model design

4. Analysis of simulation results

4.1 Analysis of the evolution process of blasting stress field

As shown in Figure 4, the effective stress evolution process of the simultaneous detonation model is shown (the time in the upper left corner of the figure represents the time after the model starts calculation).

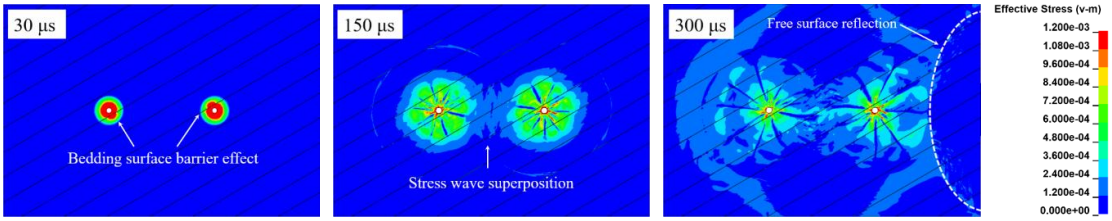

(a) Bedding rock mass

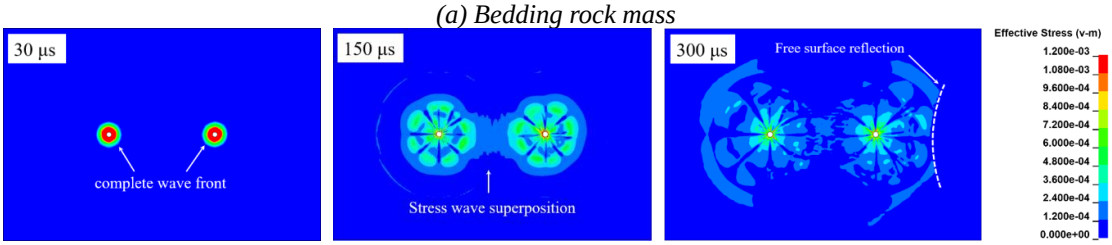

(b) Complete rock mass

Figure 4: Effective stress cloud diagram of simultaneous detonation model at different times

As can be seen from Figure 4(a), when the stress wave propagates in the layered rock mass, the closer it is to the blast center, the greater the equivalent stress intensity. At 30 μs, in the bedding rock mass, the shape of the wave front changes due to the barrier effect of bedding, while in the complete rock mass, the wave front shape is intact and circular, and the radius is about 4.8 times that of the blast hole radius by measuring the stress in the range of 120 MPa (rock compressive strength is 119.3 MPa). In the bedding rock mass, when the stress wave of the rock layer where the drug package is located is transmitted to the adjacent rock layer, reflection and transmission occur on the bedding surface, part of the stress is retained in the rock layer where the explosive is located, so that the stress strength near the blast hole is higher, and the other part of the stress penetrates the bedding into the adjacent rock layer, and the stress basically exists in the adjacent rock layer of the rock layer where the explosive is located, and is more inclined to be parallel to the direction of the bedding. At 300 μs time, the explosive stress wave emitted by the 2# blast hole has been transmitted to the free surface and reflected, because it is tensile stress, it cannot be displayed normally in the figure, but the stress distribution of the transmitted boundary and the free boundary on the left and right sides of the model can be compared, and it can be clearly observed that

ISSN 2616-5767 Vol.9, Issue 1: 24-32, DOI: 10.25236/AJETS.2026.090103

the reflected wave and the opposite direction of the incident wave lead to a decrease in the stress intensity on the side of the free plane, and the wave array is raised to the left. As a result, the stress concentration and local tensile stress of the rock mass are generated, which makes the stress in the originally low stress area increase. In order to compare the stress distribution of the detonation stress wave to the left transmission boundary of the model after the detonation of the post-detonation hole of the delayed detonation model, the stress field distribution characteristics of the model after the detonation of the 2# blast hole for 200 μs are extracted, as shown in Figure 5 (the time in the upper left corner of the figure represents the delay time of the blast hole detonation).

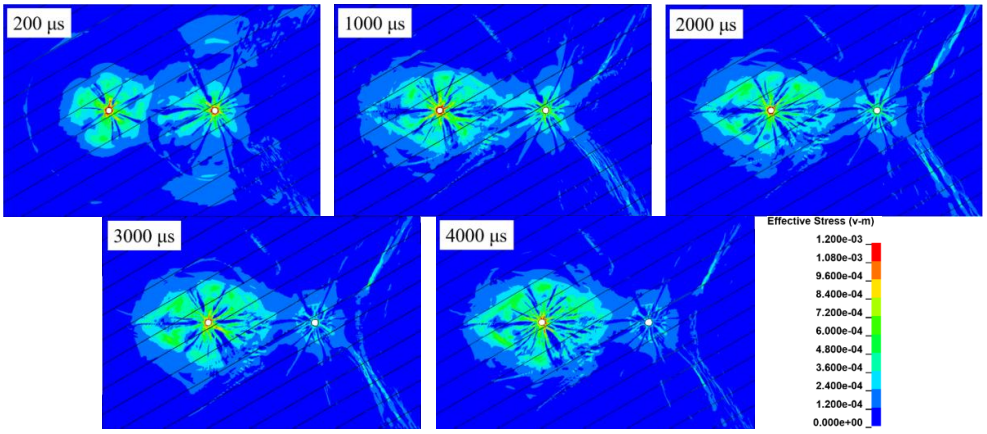

(a) Bedding rock mass

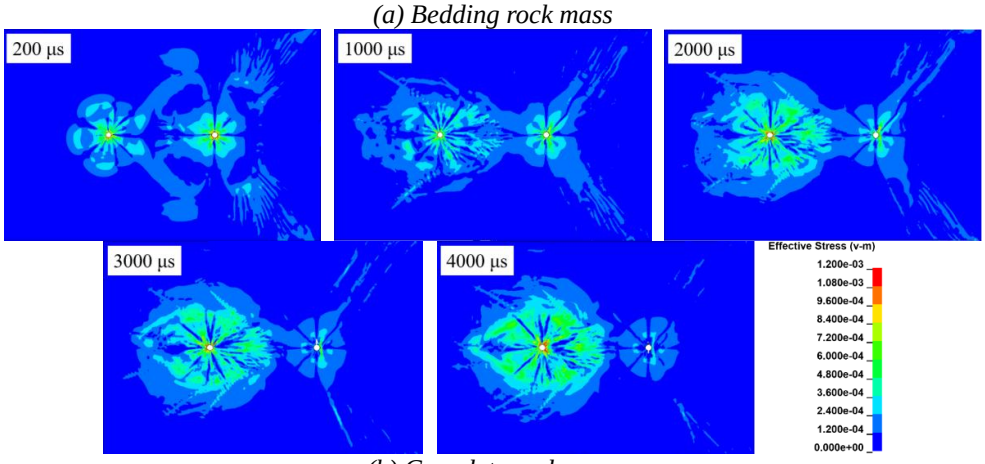

(b) Complete rock mass

Figure 5: 2# Effective stress cloud after 200 μs detonation

As can be seen from Figure 5, the 2# blast holes of each model detonated at 200, 1000, 2000, 3000 and 4000 μs, respectively, and the stress wave reflection phenomenon was formed near the free surface of each model, and with the increase of the calculation time, the stress field intensity near the 1# blast hole gradually weakened, and after the detonation of the 2# blast hole for 200 μs, it was found that most of the stress existed in the rock stratum between the 2# blast hole and the rock formation where the 1# blast hole was located and the upper adjacent rock stratum of the 2# blast hole. This is because the stress wave diffuses in the rock formation where the blast hole is located along the direction parallel to the bedding plane without being blocked, and the reflection of the stress wave in the bedding leads to part of the stress being retained in the rock layer where the blast hole is located, which also makes the radius of the wave array along this direction greater than the radius of the wave plane perpendicular to the bedding plane, and the other part of the stress passes through the bedding and enters the adjacent rock layer, and there is a certain degree of attenuation Therefore, under the action of 2# blast hole blasting, the stress concentration phenomenon will occur in this part. When the inter-hole delay is 200 μs and 1000 μs, it can be seen that the stress near the 2# blast hole of the bedding rock mass is stronger compared with the intact rock mass and the bedding rock mass, indicating that the reflection of the bedding can significantly increase the stress field strength in the near area of the blast hole. At this time, the time of 2# blast hole detonation of 200 μs is already in the time when the 1# blast hole stress wave expands the rock fracture, and it can be found that the stress concentration area perpendicular to the direction of the 1# blast hole appears on the upper and lower sides of the 2# blast hole, which is the effect of the burst crack of the 1# blast hole. With the increase of the inter-hole delay, the first blast hole blasting produces more cracks,

ISSN 2616-5767 Vol.9, Issue 1: 24-32, DOI: 10.25236/AJETS.2026.090103

which creates more favorable conditions for the detonation of the later blast hole, and the stress field strength around the 2# blast hole increases significantly.

4.2 Stress time history analysis of feature points

In order to explore the influence of stress on the bedding, four measuring points are selected from the wall of the blast hole to the adjacent rock layer between the two blast holes, and the spacing between the measuring points is 1 cm, of which measuring points I and II are in the rock formation where the blast hole is located, and measuring points III and IV are in the adjacent rock layer, as shown in Figure 6, and the stress time history diagram at different measuring points is obtained, as shown in Figure 7.

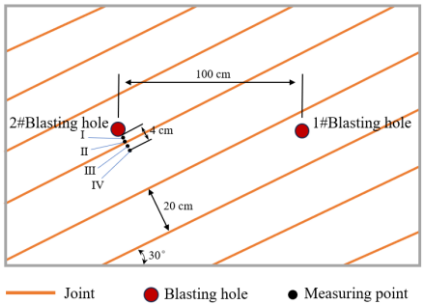

Figure 6: Location of stress measurement points

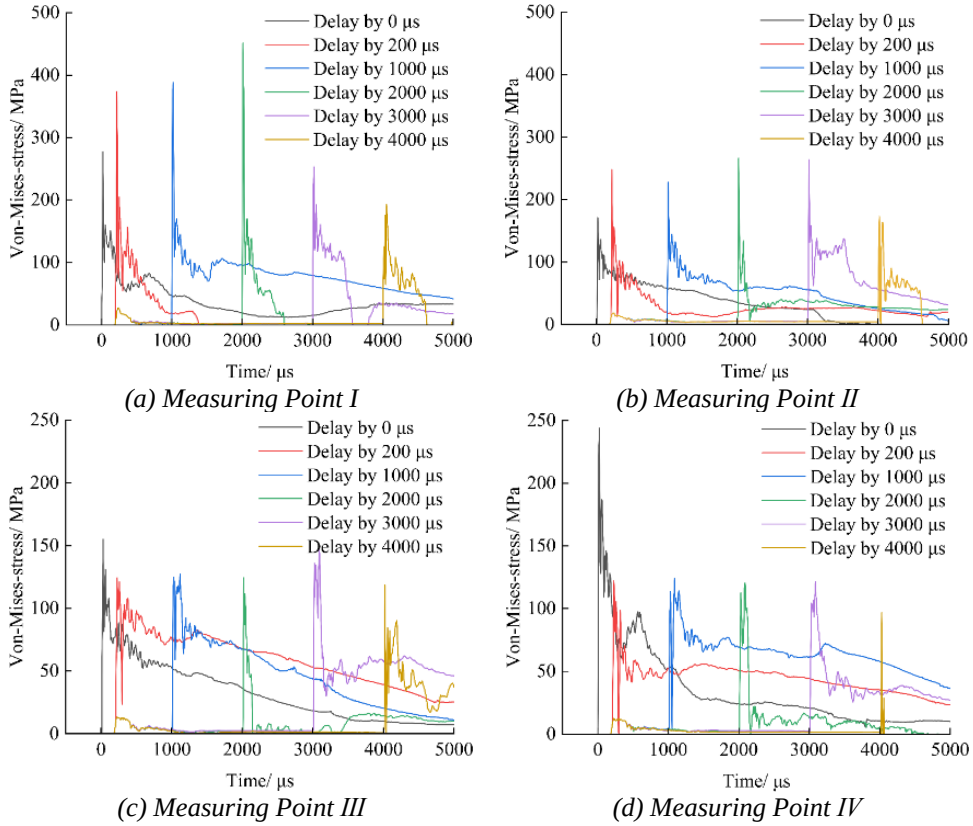

(a) Measuring Point I

(b) Measuring Point II

(c) Measuring Point III

(d) Measuring Point IV

Figure 7: Stress time history curve

It can be seen from Figure 7 that after the detonation of the 2# blast hole, the stress of the corresponding measurement points of each model quickly reaches its peak, and then decays rapidly. Due to the influence of bedding, the stress peak of the same delay time model is generally higher than that at measuring point III. and IV., and the stress peak of each model at measuring point I. is the largest, among which the model with inter-hole delay time of 2000 μs has the largest stress peak at measuring point I., reaching 457 MPa, while the stress peak of the model at measuring point IV. is only 122 MPa, which is a year-on-year decrease of 73%. It is found that the model with an inter-hole delay time of 200 μs attenuates by 54% year-on-year, the model with an inter-hole delay time of 1000 μs decreases by 63% year-on-year, the model with an inter-hole delay time of 3000 μs attenuates by 52% year-on-year, the

ISSN 2616-5767 Vol.9, Issue 1: 24-32, DOI: 10.25236/AJETS.2026.090103

model with an inter-hole delay time of 4000 μs attenuates by 48% year-on-year, and the model with an inter-hole delay time of 4000 μs has the smallest stress reduction. At 200 μs, the stress wave of the 1# blast hole is transmitted to the vicinity of the measurement point, so that the model with delay time between the holes has a slight stress increase phenomenon at each measurement point.

4.3 Analysis of blasting damage form

The final damage results of each model are exported through the post-processing software, as shown in Figure 8 (the time in the upper left corner of the figure represents the delay time of blast hole detonation).

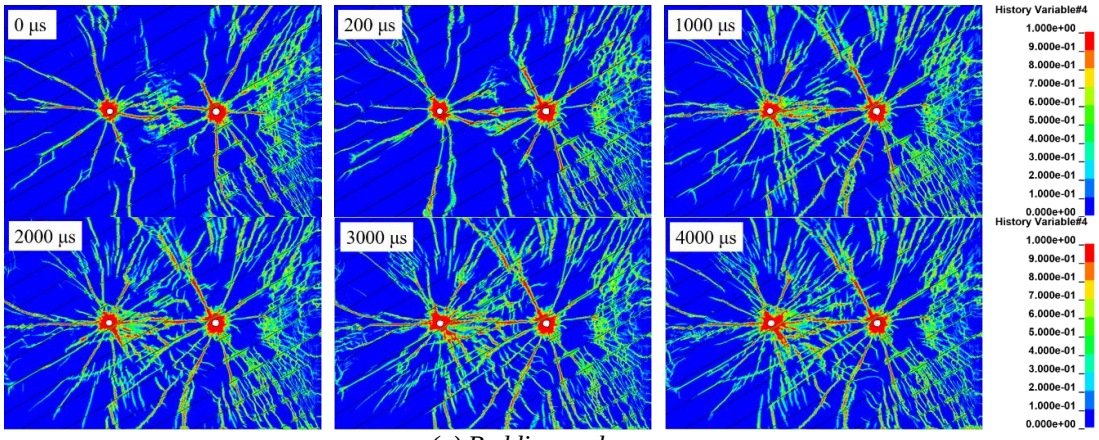

(a) Bedding rock mass

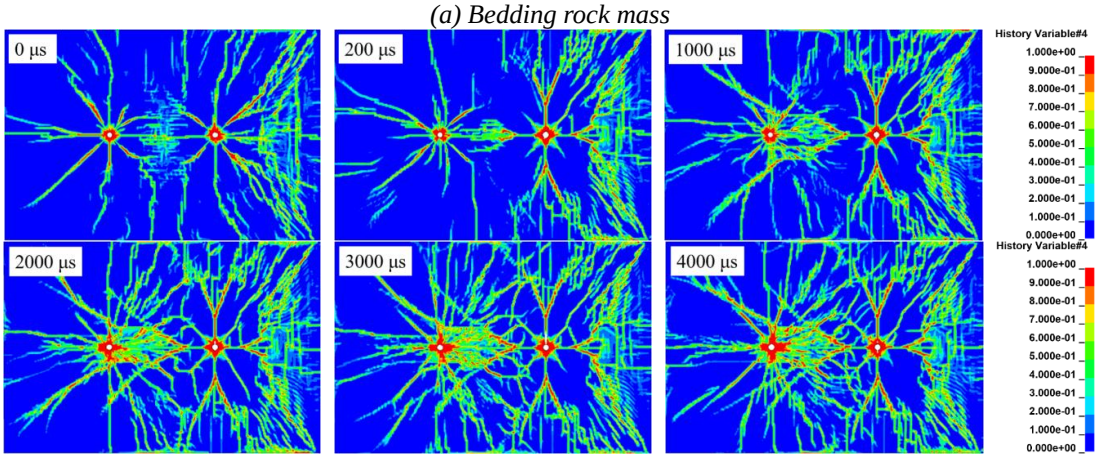

(b) Complete rock mass

Figure 8: Final damage form

With the increase of the delay time between holes, the damage degree of each model shows an increasing trend, and due to the continuous action of the first burst hole, the rock mass is continuously weakened and more cracks are formed, so that the damage effect of the post-burst hole can be further improved. Due to the action of reflective tensile stress, more tensile cracks are formed near the free surface of each model, and in the bedding rock mass, under the influence of the bedding surface, the direction of the crack is shifted to a certain extent, which generally exists near the bedding and extends in the direction of the bedding, and in the complete rock mass model, the tensile cracks near the free plane are funnel-shaped and point to the 1# blast hole. Although the damage distribution law of the bedded rock mass and the complete rock mass model is different, the crack formation mechanism is the same, and when the two holes are detonated at the same time, although the stress wave superposition can be promoted, the rock clamping effect is large, and clear penetrating cracks cannot be formed. In the model with a delay of 200 μs between holes, the damage and damage near the bedding surface in the layered rock mass between the two holes is significant, and penetrating cracks appear between the holes, and the damage units are distributed along the bedding plane on the bedding surface near the blast hole, and the damage units on the bedding surface far away from the blast hole are more distributed along the vertical bedding plane direction. When the inter-hole delay is greater than 1000 μs, the delayed detonation time between the holes is already in the time when the stress wave expands the rock fracture, and it can be clearly found that the first blast hole extends several cracks, and the clamping effect of the rock is

ISSN 2616-5767 Vol.9, Issue 1: 24-32, DOI: 10.25236/AJETS.2026.090103

greatly weakened by the auxiliary action of the fracture, and these cracks and bedding surfaces promote the reflection and stretching of the stress wave of the post-blast hole, which makes the dense cracks appear around the post-blast hole, which further improves the rock breaking efficiency of the post-blast hole. Observation Figure 8(a) and (b) show that the blasting and rock breaking effect is best when the interpore delay between the bedded rock mass and the complete rock mass model is 4000 μs.

5. Conclusion

(1) In the bedding rock mass, the stress wave transmission is obviously blocked by the bedding, and most of the stress is retained in the rock formation where the blast hole is located and the adjacent rock layer, and the reflection effect of the bedding surface improves the strength of the stress field in the rock formation near the blast hole.

(2) In the bedded rock mass, the barrier effect of the bedding plane is further reflected, and the peak attenuation of the stress at the measurement points on both sides is larger, the model with an inter-hole delay time of 2000 μs has the largest attenuation of 73%, and the model with an inter-hole delay time of 4000 μs has the smallest attenuation of only 48%.

(3) When the inter-hole delay between the bedded rock mass and the complete rock mass model is 4000 μs, the blasting and rock breaking effect is the best, and the design requirements of the delayed detonation time between the holes are consistent with that of the complete rock mass.

References

[1] Rao J Y, Xue Y H, Shen Y, et al. Analysis of correlation coupling between bedding distribution and blasting damage based on RHT model[J]. Journal of Central South University(Science and Technology), 2023, 54(3): 1204−1218.

[2] Agrawal Anurag, Choudhary B.S., Murthy V.M.S.R., et al. Impact of bedding planes, delay interval and firing orientation on blast induced ground vibration in production blasting with controlling strategies[J]. Measurement, 2022, 202.

[3] Yang G L, Bi J J, Dong Z W, et al. Fracturing mechanism of bedding shale under directional fracture-controlled blasting[J]. Explosion and Shock Waves, 2024, 44 (06): 3-17.

[4] Chen Y K, Xu J H, Huo X H, et al. Numerical Simulation of Dynamic Damage and Stability of a Bedding Rock Slope under Blasting Load[J]. Shock and Vibration, 2019, 2019: 1-13.

[5] Wang H Y, Chen X, Lu B D, et al. Influence of bedding planes on stress wave propagation in hydraulic blasting[J]. Engineering Blasting, 2022, 28 (01): 17-25.

[6] Yang R S, Ding C X, Yang L Y, et al. Blast cracking of borehole-crossed bedding under high stress condition[J]. Chinese Journal of Rock Mechanics and Engineering, 2018, 37 (04): 801-808.

[7] Xu X, Chi L Y, Zhang Z X, et al. Insight into Rock Fragmentation and Damage Affected by Temporal Characteristics of Blast Loading[J]. Rock Mechanics and Rock Engineering, 2025, 58(5): 1-23.

[8] Li H C, Chen Y, Liu D S, et al. Sensitivity Analysis Determination and Optimization of Rock RHT Parameter[J]. Transactions of Beijing Institute of Technology, 2018, 38 (08): 779-785.

[9] Xie L X, Lu W B, Zhang Q B, et al. Analysis of damage mechanisms and optimization of cut blasting design under high in situ stresses[J]. Tunnelling and Underground Space Technology, 2017, 66: 19-33.

[10] Zhang J G, Yang Wen, Wang H B, et al. The influence of angle between the bedding plane and bore hole on Smooth blasting effect of tunnels[J]. Engineering Blasting, 2025, 31(1): 24-33.

[11] Zhang F P, Peng J Y, Fan G H, et al. Mechanisms of blasting-induced rock fractures under different static stress and joint properties conditions[J]. Rock and Soil Mechanics, 2016, 37 (07): 1839-1846+1913.

[12] Zong Qi, Liu Ji M, Xu Y, et al. Theoretical Analysis and Experiment Research on Reasonable Delay Time of Millisecond Blasting [J]. Journal of China University of Mining & Technology, 1998, (01): 88-91.

[13] Fu S G, Liu Z G, Zhang J Y, et al. Study on mechanism of controlled blasting and damage evolution of rock mass under high ground stress[J]. Journal of Mining & Safety Engineering, 2024, 41 (04): 867-878.